ISSN 0031-918X, The Physics of Metals and Metallography, 2015, Vol. 116, No. 4, pp. 336–340. © Pleiades Publishing, Ltd., 2015.
Original Russian Text © S.P. Repetskii, I.G. Vyshivanaya, V.A. Skotnikov, A.A. Yatsenyuk, 2015, published in Fizika Metallov i Metallovedenie, 2015, Vol. 116, No. 4, pp. 356–360.

THEORY OF METALS

Energy Spectrum and Electrical Conductivity of Graphene with a Nitrogen Impurity

S. P. Repetskii[a], I. G. Vyshivanaya[b], V. A. Skotnikov[a], and A. A. Yatsenyuk[a]

[a] *Taras Shevchenko Kiev National University, ul. Vladimirskaya 64, Kiev, 01033 Ukraine*
[b] *Institute of High Technologies, Taras Shevchenko Kiev National University, pr. akad. Glushkova 4g, Kiev, 02033 Ukraine*
e-mail: srepetsky@univ.kiev.ua

Received July 7, 2014; in final form, November 6, 2014

Abstract—The electronic structure of graphene with a nitrogen impurity has been studied based on the model of tight binding using exchange-correlation potentials in the density-functional theory. Wave functions of 2*s* and 2*p* states of neutral noninteracting carbon atoms have been chosen as the basis. When studying the matrix elements of the Hamiltonian, the first three coordination shells have been taken into account. It has been established that the hybridization of electron-energy bands leads to the splitting of the electron energy spectrum near the Fermi level. Due to the overlap of the energy bands, the arising gap behaves as a quasi-gap, in which the density of the electron levels is much lower than in the rest of the spectrum. It has been established that the conductivity of graphene decreases with increasing nitrogen concentration. Since the increase in the nitrogen concentration leads to an increase in the density of states at the Fermi level, the decrease in the conductivity is due to a sharper decrease in the time of relaxation of the electron sates.

Keywords: nitrogen-doped graphene, electron energy spectrum, tight-binding model
DOI: 10.1134/S0031918X15040146

INTRODUCTION

One way to change graphene properties in order to apply them in nanoelectronics and spintronics is to introduce impurities of foreign elements into graphene. The presence of impurities can lead to changes in the symmetry of crystal lattice and the appearance of additional energy gaps, the width of which depends on the types of impurities and their concentrations [1–7].

The authors of [1, 2] have used a simple single-band Lifshitz model of a disordered alloy to analytically investigate the opening of the gap in the energy spectrum of electrons near the Dirac point, which takes place following an increase in the impurity concentration.

The authors of [3] used the pseudopotential method in terms of the density-functional theory to study the electronic structure of isolated monolayer, bilayer, and trilayer graphene and graphene grown on ultrathin layers of hexagonal boron nitride (h-BN). It has been shown that, in the case of a single layer of graphene on a monolayer of h-BN, a 57-meV-wide energy gap appears.

In [4], the same method was used to study graphene with impurities of aluminum, silicon, phosphorus, and sulfur. It has been shown that graphene with an impurity of 3% P has a gap 0.67 eV wide.

In [5], the electronic structure of graphene was studied in terms of the density-functional theory using the generalized gradient approximation for the exchange-correlation potential. Using the QUANTUM-ESPRESSO program package, the authors of [5] have demonstrated the possibility of opening a gap in the energy spectrum of graphene upon the introduction of atoms of boron and nitrogen (bandwidth 0.49 eV), as well as upon the introduction of boron atoms and lithium atoms adsorbed on the surface (bandwidth 0.166 eV).

In [6, 7], methods of making direct measurements of the energies of the Dirac point and Fermi energy of graphene in different heterostructures have been suggested. For graphene in a multilayered Al_2O_3/graphene/SiO_2/Si structure, the energy of the Dirac point is equal to 3.58 eV and the Fermi energy is 3.25 eV [6].

However, the effect of impurities on the electronic structure and related properties of graphene have been studied insufficiently. In this work, we have investigated the influence of nitrogen on the electronic structure and electrical conductivity of graphene based on the multiband tight-binding model.

RESULTS AND DISCUSSION

The investigations of the energy spectrum and conductivity were carried out based on the method of

cluster expansion in some small parameter for the two-time Green's functions of the electron system of a disordered crystal. As the zeroth-order single-site approximation in this method of cluster expansion, we selected the coherent-potential approach. It has been shown that the contributions of the electron scattering on clusters decrease with an increasing number of sites in the cluster [8]. In the above works, the description of the electron–electron and electron–phonon interaction is based on the Feynman diagram technique for the temperature Green's functions, which is a generalization of the well-known technique for the homogeneous electron gas [14], by applying well-known relations between the spectral representations for the temperature and two-time Green's functions.

In the calculations of the energy spectrum and electrical conductivity of nitrogen-doped graphene, real wave functions of the 2*s* and 2*p* states of neutral noninteracting carbon atoms have been chosen. The wave functions of the neutral noninteracting atoms were found from the Kohn–Sham equation in terms of the density-functional theory. The exchange-correlation potential was calculated in the meta-generalized-gradient approximation [15]. The matrix elements of the Hamiltonian were calculated by the Slater–Koster method [16] taking into account the first three coordination shells.

By neglecting the contributions from the processes of electron scattering on clusters consisting of three and greater number of atoms, which are small in the expansion in the above-mentioned parameter [8], we obtain the following relation for the density of electron states:

$$g(\varepsilon) = \frac{1}{\nu}\sum_{i,\gamma,\sigma,\lambda} P_{0i}^{\lambda} g_{0i\gamma\sigma}^{\lambda}(\varepsilon);$$

$$g_{0i\gamma\sigma}^{\lambda}(\varepsilon) = -\frac{1}{\pi}\,\mathrm{Im}\,\Big\{\tilde{G} + \tilde{G}\,t_{0i}^{\lambda}\tilde{G} + \sum_{\substack{(nj)\neq(0i)\\ \lambda'}} P_{nj0i}^{\lambda'/\lambda} \times \tilde{G}\left[t_{nj}^{\lambda'} + T^{(2)\lambda\,0i,\lambda' nj} + T^{(2)\lambda' nj,\lambda\,0i}\right]\tilde{G}\Big\}^{0i\gamma\sigma,0i\gamma\sigma}, \quad (1)$$

where i is the order number of a sublattice, ν is the number of sublattices, γ is the order number of the energy band, and σ is the quantum number of the electron-spin projection onto the z axis.

In Eq. (1),

$$T^{(2)\,n_1i_1,n_2i_2} = \left[I - t^{n_1i_1}\tilde{G}t^{n_2i_2}\tilde{G}\right]^{-1} t^{n_1i_1}\tilde{G}t^{n_2i_2}\left[I + \tilde{G}t^{n_1i_1}\right],$$

$t^{n_1i_1}$ is the operator of scattering on a single site, which is determined as follows:

$$t^{n_1i_1} = \left[I - (\Sigma^{n_1i_1} - \sigma^{n_1i_1})\tilde{G}\right]^{-1}(\Sigma^{n_1i_1} - \sigma^{n_1i_1}). \quad (2)$$

In the formula (1), P_{0i}^{λ} and $P_{nj0i}^{\lambda'/\lambda}$ are the probabilities and conditional probabilities of the placement of atoms of the λ type, respectively.

The quantity $\tilde{G} = \tilde{G}_r$ in Eqs. (1) and (2) is the retarded Green's function of the effective medium, which is described by the coherent potential $\sigma^{n_1i_1}$.

The expression for the conductivity of the system of electrons in a disordered crystal was obtained in [9–12] using the Kubo formula. Neglecting the contributions from the processes of scattering on clusters consisting of three and greater number of sites, the static conductivity can be presented as follows [11–13]:

$$\begin{aligned}\sigma_{\alpha\beta} = \frac{e^2\hbar}{4\pi V_1}\Bigg\{\int_{-\infty}^{\infty} d\varepsilon_1 \frac{\partial f}{\partial \varepsilon_1}\sum_{s,s'=+,-}(2\delta_{ss'}-1)\\ \times \sum_{\sigma\gamma,i}\Big\{[\nu_\beta \tilde{K}\left(\varepsilon_1^s,\nu_\alpha,\varepsilon_1^{s'}\right)] + \sum_{\lambda,m_{\lambda,i}} P_{0i}^{\lambda,m_{\lambda,i}}\tilde{K}(\varepsilon_1^{s'},\nu_\beta,\varepsilon_1^s)\\ \times (t_{0i}^{\lambda,m_{\lambda,i}}(\varepsilon_1^s)\tilde{K}(\varepsilon_1^s,\nu_\alpha,\varepsilon_1^{s'})t_{0i}^{\lambda,m_{\lambda,i}}(\varepsilon_1^{s'}) + \sum_{\lambda,m_{\lambda,i}} P_{0i}^{\lambda,m_{\lambda,i}}\\ \times \sum_{\substack{lj\neq 0i,\\ \lambda',m_{\lambda,j}}} P_{lj0i}^{\lambda',m_{\lambda,j}/\lambda,m_{\lambda,i}}\Big[[\tilde{K}(\varepsilon_1^{s'},\nu_\beta,\varepsilon_1^s)\nu_\alpha\tilde{G}(\varepsilon_1^{s'})]\\ \times T^{(2)\lambda,m_{\lambda,i}\;0i,\lambda',m_{\lambda,j}lj}(\varepsilon_1^{s'}) + [\tilde{K}(\varepsilon_1^{s'},\nu_\beta,\varepsilon_1^s)\nu_\alpha\tilde{G}(\varepsilon_1^{s'})]\\ \times T^{(2)\lambda',m_{\lambda,j}lj,\lambda,m_{\lambda,i}\;0i}(\varepsilon_1^{s'}) + [\tilde{K}(\varepsilon_1^s,\nu_\alpha,\varepsilon_1^{s'})\nu_\beta\tilde{G}(\varepsilon_1^s)]\\ \times T^{(2)\lambda\;m_{\lambda,i}0i,\lambda'\,m_{\lambda',j}lj}(\varepsilon_1^s) + [\tilde{K}(\varepsilon_1^s,\nu_\alpha,\varepsilon_1^{s'})\nu_\beta\tilde{G}(\varepsilon_1^s)]\\ \times T^{(2)\lambda'm_{\lambda',j}lj,\lambda,m_{\lambda,i}\;0i}(\varepsilon_1^s) + \tilde{K}(\varepsilon_1^{s'},\nu_\beta,\varepsilon_1^s)\\ \times\Big[(t_{lj}^{\lambda'm_{\lambda',j}}(\varepsilon_1^s)\tilde{K}(\varepsilon_1^s,\nu_\alpha,\varepsilon_1^{s'})t_{0i}^{\lambda,m_{\lambda,i}}(\varepsilon_1^{s'})\\ + t_{lj}^{\lambda'm_{\lambda',j}}(\varepsilon_1^s)\tilde{K}(\varepsilon_1^s,\nu_\alpha,\varepsilon_1^{s'})T^{(2)\lambda\;m_{\lambda,i}0i,\lambda'm_{\lambda',j}lj}(\varepsilon_1^{s'})\\ + T^{(2)\lambda'm_{\lambda',j}lj,\lambda,m_{\lambda,i}\;0i}(\varepsilon_1^s)\tilde{K}(\varepsilon_1^s,\nu_\alpha,\varepsilon_1^{s'})t_{0i}^{\lambda,m_{\lambda,i}}(\varepsilon_1^{s'})\\ + T^{(2)\lambda'm_{\lambda',j}lj,\lambda,m_{\lambda,i}\;0i}(\varepsilon_1^s)\tilde{K}(\varepsilon_1^s,\nu_\alpha,\varepsilon_1^{s'})T^{(2)\lambda,m_{\lambda,i}\;0i,\lambda'm_{\lambda',j}lj}(\varepsilon_1^{s'})\\ + T^{(2)\lambda'm_{\lambda',j}lj,\lambda,m_{\lambda,i}\;0i}(\varepsilon_1^s)\tilde{K}(\varepsilon_1^s,\nu_\alpha,\varepsilon_1^{s'})\\ \times T^{(2)\lambda'm_{\lambda',j}lj,\lambda,m_{\lambda,i}\;0i}(\varepsilon_1^{s'}))\Big]\Big]\Big\}^{0i\gamma\sigma,0i\gamma\sigma}\\ + \int_{-\infty}^{\infty}\int_{-\infty}^{\infty} d\varepsilon_1 d\varepsilon_2 f(\varepsilon_1) f(\varepsilon_2)\left\langle\Delta G_{\alpha\beta}^{\mathrm{II}}(\varepsilon_1,\varepsilon_2)\right\rangle\Bigg\},\end{aligned} \quad (3)$$

where $\tilde{K}\left(\varepsilon_1^s,\nu_\alpha,\varepsilon_1^{s'}\right) = \tilde{G}\left(\varepsilon_1^{s'}\right)\nu_\alpha\tilde{G}\left(\varepsilon_1^{s'}\right)$;

$$\tilde{G}\left(\varepsilon_1^+\right) = \tilde{G}_r(\varepsilon_1)\;\tilde{G}\left(\varepsilon_1^-\right) = \tilde{G}_a(\varepsilon_1) = \left(\tilde{G}_r\right)^*(\varepsilon_1),$$

$f(\varepsilon)$ is the Fermi function, V_1 is the volume of a primitive cell, e is the electron charge, and $\hbar$ is Planck's constant.

The quantity $\Delta G_{\alpha\beta}^{\mathrm{II}}(\varepsilon_1,\varepsilon_2)$ in Eq. (3) is a composite two-particle Green's function, which is expressed through a vertex function of the mass operator of the electron–electron interaction [11]. As follows from numerical calculations, the contribution from the last

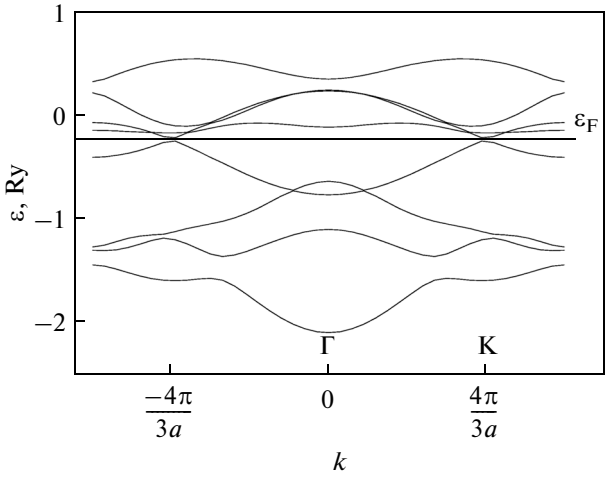

Fig. 1. Electron energy spectrum of pure graphene.

term to (3) does not exceed a few percent; therefore, we neglected this contribution in our calculations.

The operator of the α projection of the electron velocity ν_α in (3) is written as follows:

$$\nu_{\alpha i,i'}(\mathbf{k}) = \frac{1}{\hbar}\frac{\partial h_{i,i'}(\mathbf{k})}{\partial k_\alpha}.$$

The calculations of the energy spectrum and conductivity of graphene have been performed for the temperature $T = 0$ K.

Figure 1 displays the dependence of the electron energy ε in pure graphene on the wave vector **k**, which was obtained from the condition for the poles of the Green's function. The vector **k** is directed from the center of the Brillouin zone (point Γ) to the Dirac point (point K).

In Fig. 1, $a = \sqrt{3}a_0$, where $a_0 = 0.142$ nm is the shortest spacing between carbon atoms.

Figures 2 and 3 display the energy dependences of the electron states $g(\varepsilon)$ (1) of graphene with an nitrogen impurity atoms. The solid vertical lines in these figures show the positions of the Fermi level. Figure 3 shows part of the energy spectrum in the vicinity of the Fermi level.

As can be seen from Figs. 1–3, the hybridization leads to the appearance of an energy gap in the band, which is caused by the ($pp\pi$) bond [16]. The electron states in this band are described by atomic wave functions of z symmetry. The Fermi level is located in the middle of the gap; its magnitude corresponds to the position of the Dirac point. The width of the band is equal to 0.08 Ry, i.e., about 1 eV. The position of the Fermi level corresponds to the energy $\varepsilon_F = -0.23$ Ry $\approx$ −3.13 eV. Due to the overlap of the bands, the gap behaves as a quasi-gap in the energy spectrum of electrons. The density of electron states in the region of this gap is significantly less than the density of states in neighboring regions of the spectrum (Fig. 2). The position of the Fermi level depends on the nitrogen concentration and is located in the range of -0.36 Ry $\le \varepsilon_F \le -0.23$ Ry. The quasi-band width decreases with increasing nitrogen concentration and the Fermi level is shifted toward the left-hand edge of the spectrum. The theoretical values of the Fermi level for pure graphene are in agreement with the experimental values for graphene in a multilayered Al_2O_3/graphene/SiO_2/Si structure [6].

Figure 4 shows the concentration dependence of the components of the tensor of static conductivity $\sigma_{\alpha\beta}$ of graphene calculated via (2) at $T = 0$ K. The x axis is directed toward the nearest-neighbor atom. As can be seen from the figure, the conductivity of graphene decreases with increasing nitrogen concentration.

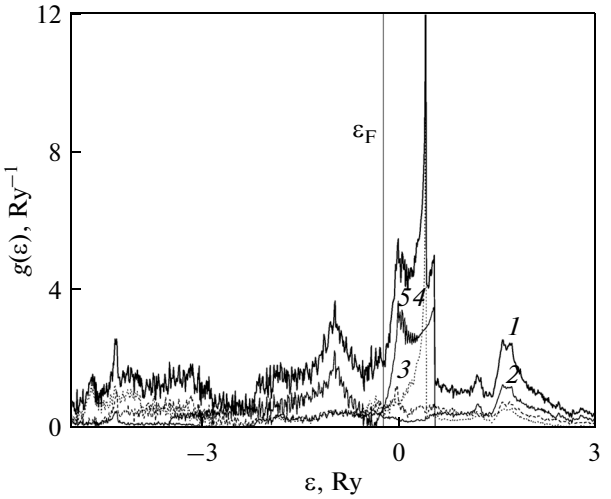

Fig. 2. Density of electron states $g(\varepsilon)$ of graphene with an impurity of 1% nitrogen: (*1*) total density of states. The partial components are (*2*) 2*s*, (*3*) $2p_x$, (*4*) $2p_y$, and (*5*) $2p_z$.

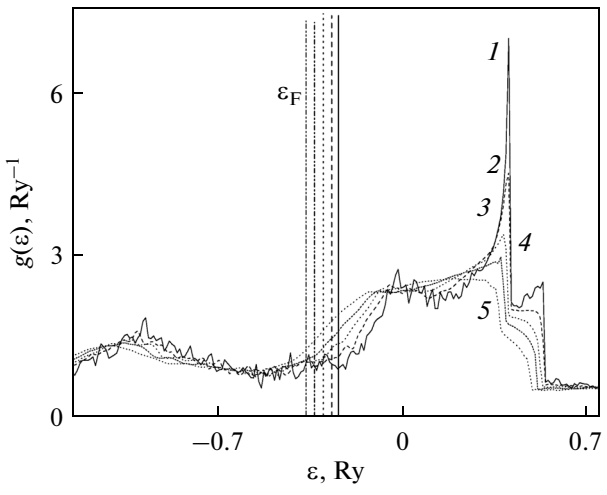

Fig. 3. Densities of electron states $g(\varepsilon)$ of nitrogen-doped graphene: (*1*) 1, (*2*) 3, (*3*) 5, (*4*) 7, and (*5*) 10 at % nitrogen.

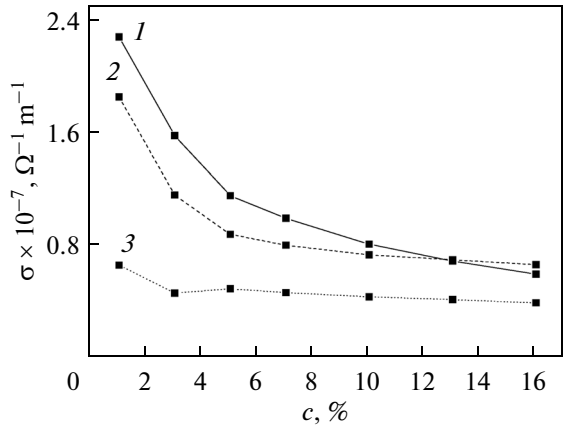

Fig. 4. Dependence of the components of the conductivity tensor on the concentration of nitrogen c: (*1*) σ_{xx}, (*2*) σ_{yy}, and (*3*) σ_{xy}.

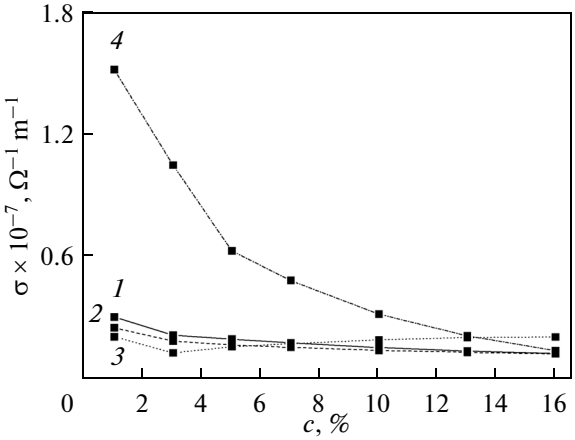

Fig. 5. Dependences of the 2*s* and 2*p* partial components of the σ_{xx} component of the conductivity tensor on the impurity concentration c: (*1*) 2*s*, (*2*) $2p_x$, (*3*) $2p_y$, and (*4*) $2p_z$.

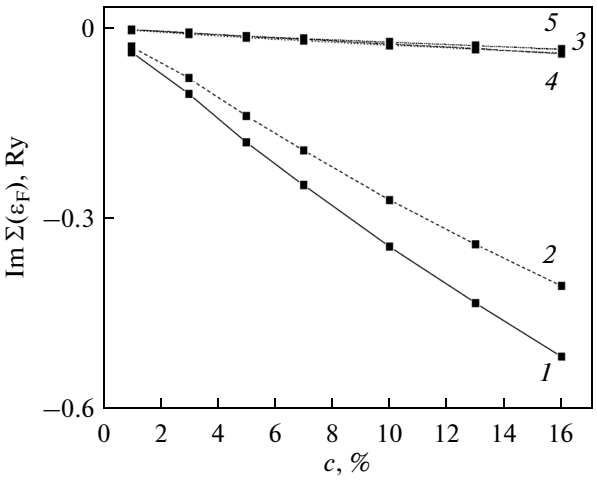

Fig. 6. Dependences of the total and 2*s* and 2*p* partial components of the imaginary part of the mass operator of the Green's function of graphene on the concentration c of the nitrogen impurity: (*1*) imaginary part of the mass operator; partial components: (*2*) 2*s*, (*3*) $2p_x$, (*4*) $2p_y$, and (*5*) $2p_z$.

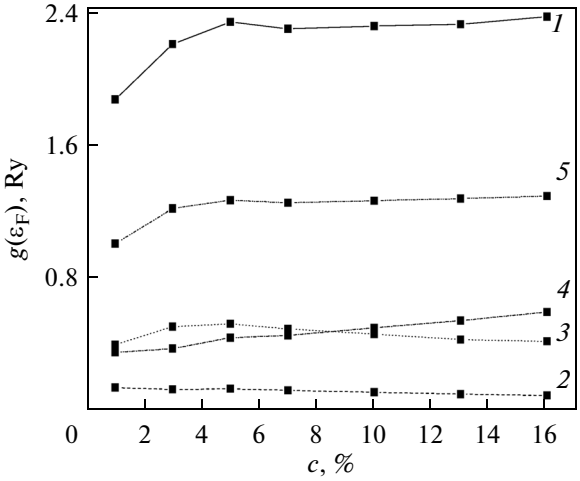

Fig. 7. Dependences of the total and 2*s* and 2*p* partial components of the density of electron states $g(\varepsilon_F)$ at the Fermi level of graphene on the concentration c of nitrogen impurity: (*1*) total density of states; partial components: (*2*) 2*s*, (*3*) $2p_x$, (*4*) $2p_y$, and (*5*) $2p_z$.

For comparison, we give the experimental value of the conductivity of graphite; at 300 K, it is equal to 9.82×10^5 Ω^{-1} m^{-1} [17].

Figure 5 demonstrates the concentration dependence of the 2*s* and 2*p* partial components of the σ_{xx} component of the tensor of static conductivity. It can be seen that the main contribution to the conductivity comes from the electron states that are described by the atomic wave functions $2p_z$ [16].

In order to investigate the nature of the concentration dependence of the conductivity, let us consider a limiting expression for the case of weak scattering, which follows from the general Eq. (3) in the single-band approximation shown below [12]:

$$\sigma_{\alpha\alpha} = \frac{e^2\hbar}{3\Omega_1} \frac{g(\varepsilon_F) v^2(\varepsilon_F)}{|\Sigma''(\varepsilon_F)|}.$$

Here, $\Sigma''(\varepsilon_F) = \mathrm{Im}\,\Sigma(\varepsilon_F)$ is the imaginary part of the mass operator of the Green's function, $v(\varepsilon_F)$ is the electron velocity at the Fermi level, and Ω_1 is the volume per atom. The relaxation time of electron states $\tau(\varepsilon_F)$ is determined by the relation $|\Sigma''(\varepsilon_F)|\tau(\varepsilon_F) = \hbar$.

Figure 6 displays the concentration dependence of the total and 2*s* and 2*p* partial components of the imaginary part of the mass operator of the Green's function.

Figure 7 shows the concentration dependence of the total and 2*s* and 2*p* partial components of the density of electron states at the Fermi level.

As can be seen from Figs. 6 and 7, the main contribution to the conductivity comes from the $2p_z$ partial component.

Since the density of electron states at the Fermi level increases with increasing nitrogen concentration (Fig. 7), the decrease in the conductivity observed in Figs. 4 and 5 is explained by a sharper decrease in the relaxation time of the electron states (Fig. 6).

REFERENCES

1. Yu. V. Skrypnyk and V. M. Loktev, "Impurity effects in a two-dimensional system with the Dirac spectrum," Phys. Rev. B: Condens. Matter Mater. Phys. **73**, 241402 (2006).
2. Yu. V. Skrypnyk and V. M. Loktev, "Local spectrum rearrangement in impure graphene," Phys. Rev. B: Condens. Matter Mater. Phys. **75**, 245401 (2007).
3. C. Yelgel and G. P. Srivastava, "Ab initio studies of electronic and optical properties of graphene and graphene–BN interface," Appl. Surf. Sci. **258**, 8338–8342 (2012).
4. Pablo A. Denis, "Band gap opening of monolayer and bilayer graphene doped with aluminum, silicon, phosphorus, and sulfur," Chem. Phys. Lett. **492**, 251–257 (2010).
5. D. Xiaohui, W. Yanqun, D. Jiayu, K. Dongdong, and Z. Dengyu, "Electronic structure tuning and band gap opening of graphene by hole/electron codoping," Phys. Lett. A. **365**, 3890–3894 (2011).
6. K. L. Xu, C. Zeng, Q. Zhang, R. Yan, P. Ye, K. Wang, A. C. Seabaugh, H. G. Xing, J. S. Suehle, C. A. Richter, D. J. Gundlach, and N. V. Nguyen, "Direct measurement of Dirac point energy at the graphene/oxide interface," Nano Lett. **13**, 131–136 (2013).
7. S. Kim, I. Jo, D. C. Dillen, D. A. Ferrer, B. Fallahazad, Z. Yao, S. K. Banerjee, and E. Tutuc, "Direct measurement of the Fermi energy in graphene using a double-layer heterostructure," Phys. Rev. Lett. **108**, 116404 (2012).
8. S. P. Repetsky and T. D. Shatnii, "Thermodynamic potential of a system of electrons and phonons in a disordered alloy," Theor. Math. Phys. **131**, 456–478 (2002).
9. S. P. Repetsky and I. G. Vyshivanaya, "Optical conductivity of disordered alloys and semiconductors," Metallofiz. Nov. Tekhnol. **26**, 887–909 (2004).
10. S. P. Repetsky and I. G. Vyshivanaya, "Optical Conductivity of Ordering Alloys," Phys. Met. Metallogr. **99**, 558–566 (2005).
11. S. P. Repetsky and I. G. Vyshivanaya, "Electrical conductivity of magnetically ordered crystals," Metallofiz. Noveishie Tekhnol. **29**, 587–610 (2007).
12. S. P. Repetsky, I. G. Vyshivanaya, V. V. Shastun, and A. F. Mel'nik, "Energy spectrum of electrons and phonons and electrical conductivity of carbon nanotubes with addition of nitrogen," Metallofiz. Noveishie Tekhnol. **33**, 425–445 (2011).
13. S. P. Repetsky, O. V. Tretyak, I. G. Vyshivanaya, and V. V. Shastun, "Self-consistent model of strong coupling theory of electron correlations in disordered crystals," Usp. Fiz. Met. **13**, 189–223 (2012).
14. A. A. Abrikosov, L. P. Gor'kov, and I. E. Dzyaloshinskii, *Quantum Field Theoretical Methods in Statistical Physics* (Fizmatgiz, Moscow, 1962; Pergamon, New York, 1965).
15. Jianwei Sun, Martijn Marsman, Gábor I. Csonka, Adrienn Ruzsinszky, Pan Hao, Yoon-Suk Kim, Georg Kresse, and John P. Perdew, "Self-consistent meta-generalized gradient approximation within the projector-augmented-wave method," Phys. Rev. B: Condens. Matter Mater. Phys. **84**, 035117 (2011).
16. J. C. Slater and G. F. Koster, "Simplified LCAO method for the periodic potential problem," Phys. Rev. **94**, 1498–1524 (1954).
17. A. R. Ubbellode and F. A. Lewis, *Graphite and Its Crystalline Compounds* (Oxford Univ. Press, Oxford, 1960; Mir, Moscow, 1965).

Translated by S. Gorin